Published in final edited form as:
J Pharm Sci. 2012 March ; 101(3): 1028–1039. doi:10.1002/jps.22822.

On Quantitative Relationships Between Drug-Like Compound Lipophilicity and Plasma Free Fraction in Monkey and Human

SAMI S. ZOGHBI[1], **KACEY B. ANDERSON**[1], **KIMBERLY J. JENKO**[1], **DAVID A. LUCKENBAUGH**[2], **ROBERT B. INNIS**[1], and **VICTOR W. PIKE**[1]

[1]Molecular Imaging Branch, National Institute of Mental Health, National Institutes of Health, Bethesda, Maryland 20892

[2]Therapeutics and Pathophysiology Branch, National Institute of Mental Health, National Institutes of Health, Bethesda, Maryland 20892

Abstract

Drug interactions with plasma proteins influence their pharmacokinetics and pharmacodynamics. We aimed to test whether a strong quantitative relationship exists between plasma free fraction (f_P) and lipophilicity for low molecular weight nonacidic drug-like compounds. We measured the *n*-octanol-buffer distribution coefficients at pH 7.4 ($^m\log D$) of 18 diverse radiotracers (<470 Da) used for brain imaging with positron emission tomography in vivo. Lipophilicities were also computed as $^c\log D$ with two software packages. The f_P values for monkeys and humans were determined by ultrafiltration and transformed into $^m\log D_{pr/pl}$ values representing the $\log_{10}$ of the within phase partition of the radiotracers between plasma proteins and remaining plasma. $^m\log D_{pr/pl}$ correlated strongly with $^m\log D$ for human ($^m\log D_{pr/pl} = 0.733\,^m\log D - 0.780$, $r^2 = 0.74$) and monkey ($^m\log D_{pr/pl} = 0.780\,^m\log D - 1.15$, $r^2 = 0.83$), but less strongly with $^c\log D$. These relationships were significantly different between species ($P = 0.006$). Removal of eight fluorinated compounds from the datasets raised r^2 to 0.81 and 0.91 for humans and monkeys, respectively. For the tested compounds, we conclude that *n*-octanol-buffer (pH 7.4) distribution strongly models that between plasma proteins and remaining plasma and moreover that $^m\log D$ accounts for over 74% of compound $^m\log D_{pr/pl}$ and is a strong determinant of f_P.

Keywords

Protein binding; drug-like properties; physicochemical properties; log*P*; structure-property relationship; lipophilicity; drug; radiotracer; log*D*; plasma free fraction

INTRODUCTION

The interaction of administered drugs with plasma proteins has long been of interest, since essentially only unbound drug is capable of traversing biological membranes to exert pharmacological action.[1,2] Furthermore, the extent to which a drug binds to plasma proteins will influence its distribution, rate of metabolism, and excretion.[1,2] In our laboratory, we are primarily interested in developing and applying radiotracers (radiopharmaceuticals) for imaging protein targets within brain with the technique of positron emission tomography (PET). Commonly, such radiotracers are structurally related to central nervous system drugs. The penetration of such radiotracers across the blood–brain barrier after intravenous

Correspondence to: Sami S. Zoghbi (Telephone: 301-435-7911; Fax: 301-480-3610; sami.zoghbi@nih.gov); Victor W. Pike (Telephone: 301-594-5986; Fax: 301-480-5112; pikev@mail.nih.gov).

administration depends on many factors,[3–5] including the plasma free fraction (f_p), which may be defined as the fraction of drug in plasma that is not bound to plasma proteins.[6] For detailed pharmacokinetic analysis of the behavior of PET radiotracers aimed at deriving important imaging output parameters, accurate unbiased measurement of f_p may be required in subjects under study, whether animal or human.[6] In view of the aforementioned considerations, the interaction of drug-like compounds with plasma proteins[7,8] and the prediction of these interactions[9,10] have merited considerable study. Lipophilicity has long been recognized as an important property influencing many aspects of drug–protein interactions, and consequently drug pharmacokinetic and pharmacodynamic behavior.[1] The most widely used index of drug lipophilicity is the *n*-octanol-water partition coefficient *P*, usually expressed as $\log_{10}$ of this value ($\log P$).[11,12] As many drugs also exist in ionized forms at physiological pH (pH 7.4), the $\log_{10}$ of the partition of all forms of the drug between *n*-octanol and buffer at pH 7.4 ($\log D$) is usually considered more relevant to physiological phenomena. Nowadays, estimates of lipophilicity may be computed from simple depictions of drug structure with various commercially available software packages to give the corresponding parameters $^{c}\log P$ and $^{c}\log D$.* Because of the great ease of these computations, $^{c}\log P$ and $^{c}\log D$ values have become quite prevalent in the literature, especially for large datasets where alternative experimental determinations would be laborious.

The extent to which $\log D$ can represent the interactions of drugs with plasma proteins is a fundamental and well-discussed question.[10] Many experimental studies have observed or have derived different relationships between $\log D$ and f_p for various types of dataset. For example, Lázníček et al.[13] studied the plasma protein binding of organic acids across three animal species and humans and established relationships of the type $f_p = 1/(1 + aD^b)$, where *a* depends on species and *b* is approximately equal to 1. van de Waterbeemd et al.[14] found sigmoidal relationships between plasma protein binding (i.e., $1-f_p$) and $\log D$ that were appreciably dissimilar among acidic, basic, and neutral compounds. Laruelle et al.[4] reported a strong linear relationship between f_p and $\log P$ for a small set ($n = 4$) of congeneric imaging radiotracers. However, Saiakhov et al.[15] found a poor linear relationship ($r^2 = 0.279$) between $1-f_p$ and $\log P$ ($\log K_{ow}$) for a large dataset ($n = 154$) of diverse drugs. Yamazaki and Kanaoka[16] found strong nonlinear relationships between $^{c}\log D$ and plasma protein binding among quite large datasets of diverse basic, neutral, and acidic pharmaceuticals. By contrast, Kratochwil et al.[17] found poor correlations among a large set of both acidic and basic drugs between $\log D$ and binding affinity to human serum albumin, the most prevalent protein in plasma.

We are interested in testing the extent to which lipophilicity accounts for f_p among nonacidic PET radiotracers produced for brain imaging in our laboratory, because an understanding of the quantitative relationship between lipophilicity and its possible species dependence could be useful in further PET radiotracer development. Moreover, reliable quantification of the role of lipophilicity in drug–plasma protein interactions may be generally useful for drug design, and also facilitate the development of *in silico* predictive methods.[10,15,18,19]

In this study, we examined the relationship between f_p and lipophilicity for a moderately sized set of well-diversified low molecular weight nonacidic compounds. These compounds serve in our laboratory as radiotracers for brain molecular imaging with PET and their availability in radioactive form and in high radiochemical purity facilitated f_p and lipophilicity measurements, and provided opportunity to study the relationships between these two parameters. We found that the $\log_{10}$ of compound partition between plasma

*In this paper we use the prefix ^{c} to indicate computed value and the prefix ^{m} to indicate measured value.

proteins and the remainder of plasma correlates strongly with measured log*D* value in both the human and the monkey. Accordingly, log*D* is the major determinant of f_P in both species, and may be considered a useful parameter for the *prima facie* estimation of f_P for candidate nonacidic low molecular weight drugs or indeed brain imaging radiotracers.

MATERIALS AND METHODS

Statistics

Linear regression analysis between one dependent and one independent variable was performed by the least squares method with GraphPad Prism for Windows software (GraphPad Software; San Diego, California). Statistical significance for the uppertail *F*-test was set at the 5.0% level ($\alpha = 0.05$) for the appropriately calculated degrees of freedom. Regression lines and associated 95% confidence intervals were plotted with GraphPad Prism for Windows software. Analysis of covariance was used to test the hypothesis of whether two regression lines were equivalent. Significance of the test was performed at the 5% level ($\alpha = 0.05$). Student's *t*-test was used to test for differences in means of two samples.

Compound Selection and Preparation

Eighteen compounds for study were selected from among the radiotracers being produced in our laboratory for PET brain imaging experiments in monkey and human subjects. These compounds were labeled with either short-lived carbon-11 ($t_{1/2}$ = 20.4 min) or fluorine-18 ($t_{1/2}$ = 109.7 min) and obtained in high radiochemical purity (>99%), as described previously.[20–36] All were radiochemically stable in monkey and human plasma, except [^{18}F]SP203, which is unstable in monkey plasma.[23] The radiotracers are all low molecular weight (260–470 Da) nonacidic compounds with low total polar surface area (tPSA; range: 30–65 Å) (Table 1). They span a wide range of lipophilicity (Table 1), and represent 12 distinct core structural classes (Chart 1). Eight of the compounds contain one or more fluorine atoms. Most of the compounds are quite basic (Table 1) and exist as interconverting neutral (non-zwitterionic) and positively charged species at physiological pH (pH 7.4).

Estimation of Compound pK_a

Estimates of compound pK_a were obtained with Pal-las 3.70 software (Compudrug, S. San Francisco, California).

Computation and Measurement of Compound Lipophilicity

Pallas 3.70 software and also ACD software (version 9.04; Advanced Chemistry Development, Inc.; Toronto, Canada) were used to compute two compound lipophilicity parameters, $^{c}\log D$ (the $\log_{10}$ of compound partition between *n*-octanol and buffer at pH 7.4), and $^{c}\log P$ (the partition of the neutral compound microspecies between *n*-octanol and water). Each software uses the depicted two-dimensional structure of the compound as input for computation.

Compound lipophilicity was also measured using the radiotracer as the $\log_{10}$ of its partition between *n*-octanol and sodium phosphate buffer (pH 7.4, 0.15 M) ($^{m}\log D$) at room temperature, according to a previously published method.[29] The mean and standard deviation of six lipophilicity measurements are reported for each compound (Table 1). Computed ($^{c}\log D$) and measured ($^{m}\log D$) values were each correlated to $^{m}\log D_{pr/pl}$ by regression analysis.

Measurement of Compound Plasma Free Fraction

All animal studies were performed in accordance with the *Guide for the Use of Laboratory Animals*[37] and the National Institutes of Health Animal Care and Use Committee. Thirteen rhesus monkeys (*Macaca mulatta*) were used. All experiments involving humans were approved by the Institutional Research Board of the NIH. The f_p of each compound was measured with a radiotracer of greater than 99% radiochemical purity at room temperature in either arterial monkey or human plasma, or both. Monkey plasma was prepared from blood taken from fasted male animals that had been immobilized with ketamine and that were maintained in anesthesia with about 1.5% isoflurane in oxygen in readiness for PET imaging experiments. Human plasma was prepared from blood taken from consenting conscious adults preceding radiotracer injection for PET imaging experiments, or, in a few exceptional cases, from pooled human blood that had been stored at −70°C, as indicated in Table 1. Each determination of f_p entailed addition of radiochemically pure radiotracer (20–70 μCi), as a solution in saline or saline–ethanol (2–10 μL), to a prepared non-radioactive plasma sample (≈650 μL) followed by mixing and measure ments of f_p on three aliquots (200 μL each) by ultrafiltration (Centrifree; Millipore, Billerica, Massachusetts), as detailed previously.[38] The mean value constituted one measurement. This procedure was performed thrice for each radiotracer and the results expressed as mean ± SD for the three measurements (Table 1). Except where pooled blood was used, no animal or human contributed to more than one of the three measurements. Because of the frequency of PET experiments, f_p data were sometimes available for some radiotracers in more than three subjects. In such cases, in order to achieve equal weighting of data between radiotracers, three values were selected randomly, that is, by lottery with replacement.

Relationship of Within-Phase Partition of Compound Between Plasma Proteins and Remaining Plasma to Lipophilicity

Compound f_p values for monkey and human were transformed into within-phase partition coefficients between plasma proteins and remaining plasma ($D_{pr/pl}$), where $D_{pr/pl} = (1-f_p)/f_p$ and expressed as $\log_{10}$ of this value ($^m\log D_{pr/pl}$) (Fig. 1). For each species, these values were then correlated by regression analysis with $^c\log P$, $^c\log D$, or $^m\log D$ as independent variables. Compound datasets were also divided into those for fluorine-containing ($n = 8$) and nonfluorine-containing radiotracers ($n = 10$), and the data reanalyzed.

RESULTS AND DISCUSSION

In this study, our main findings were strong quantitative but species-distinct linear relationships between measured compound lipophilicity ($^m\log D$) and the parameter $^m\log D_{pr/pl}$ derived from our measurements of f_p in both human and nonhuman primate plasma. $^m\log D_{pr/pl}$ represents the $\log_{10}$ of the equilibrium partition of compound between plasma proteins and remaining plasma and is a parameter that may be considered analogous to the $\log_{10}$ of the equilibrium partition of compound between *n*-octanol and pH 7.4 buffer ($\log D$) (Fig. 1).

At the outset of this study, we were interested in how well commercial software might predict $\log D$ as a measure of compound lipophilicity, because computations are easily performed from simple two-dimensional structural representations. Use of the radiotracers generally allowed compound lipophilicities to be measured with high precision across a wide range of values as evident from the associated relatively small standard deviations, except for compounds **4** and **12**, which gave 10% and 11% coefficient of variance, respectively (Table 1). Compound $\log D$ values, when computed with either Pallas or ACD software and compared with measured values, showed regression lines with regression coefficients (slopes) greater than unity, but only moderately strong correlations (Fig. 2;

Table 2, entries 1 & 2). Lipophilicity (log*D*) computed from ACD software correlated somewhat more strongly with measured lipophilicity ($^{m}\log D$) (r^2 = 0.740) than did lipophilicity computed from Pallas software (r^2 = 0.619). (It should be noted that the results from each software package are not expected to correspond because they apply different methods to calculate lipophilicity from two-dimensional structure). Although these correlations may be considered to be strong, these computational methods clearly fail to predict very accurate values. In fact, for ACD and Pallas software, the root mean squared errors were 0.76 and 0.80 $\log_{10}$ units, respectively. Our observations are similar to those of Tetko and Poda[39] who, with the use of versions of Pallas, ACD and other software packages, found high root mean squared errors of 1.0 to 1.5 $\log_{10}$ units in the estimation of log*D* among very large datasets (17,861 and 640) of diverse organic compounds.

Nevertheless, we proceeded to test whether $^{c}\log D$ from either software program might correlate with $^{m}\log D_{\mathrm{pr/pl}}$ in monkey and human plasma. The use of the radiotracers allowed for quite precise determinations of compound f_{P} and the derived parameter $^{m}\log D_{\mathrm{pr/pl}}$ across a wide range of values as evident from the associated relatively small standard deviations (Table 1). From either program, significant correlations were found between $^{c}\log D$ and $^{m}\log D_{\mathrm{pr/pl}}$ for monkey and human (Fig. 3, Table 2, entries 3–6). Slopes of the regression lines were much lower than unity and the correlation coefficients were not especially high (Table 2). The ACD software gave a somewhat stronger correlation (r^2 = 0.553; Table 2, entry 3) for the human data than the Pallas software (r^2 = 0.426; Table 2, entry 5).

Because the partition coefficient of uncharged compound between *n*-octanol and water (log*P*) is also readily computed from a two-dimensional representation of compound structure, and without the need for an additional uncertain internal estimation of compound pK_{a}, we also tested for correlation between $^{c}\log P$ and $^{m}\log D_{\mathrm{pr/pl}}$ in each species. Significant correlations were found. However, correlation coefficients were found to be weaker than for $^{c}\log D$ (Table 2, c.f. entries 7 & 8), except in the case of monkey $^{m}\log D_{\mathrm{pr/pl}}$ versus $^{c}\log P$ from ACD software, which gave an almost negligible improvement (r^2 = 0.574 versus 0.569; Table 2, c.f. entries 8 and 6). Only in the single case of lipophilicity calculated with Pallas software and for the monkey data did we find that $^{c}\log P$ was appreciably more sensitive than $^{c}\log D$ to changes in $^{m}\log D_{\mathrm{pr/pl}}$ (Table 2, c.f. entries for *m* in 10 and 6). Overall, we concluded that $^{c}\log D$ gave stronger correlations than $^{c}\log P$ with $^{m}\log D_{\mathrm{pr/pl}}$ for our datasets. Our findings may be compared with those of Lobell and Sivarajah[18] for human and uncharged (i.e., neutral) and positively charged sets of compounds with molecular weights <825 Da. They found linear relationships between $^{m}\log D_{\mathrm{pr/pl}}$ and AlogP98, where the latter was a log*P* value computed with QSAR+ module of Cerius2 (version 4.6, Acclerys Inc. San Diego, California). Regression lines had similar regression coefficients ($m \approx 0.45$) to those found in this study for neutral and basic compounds (Table 3). Their large datasets gave somewhat higher correlation coefficients ($r^2 \leq 0.67$) (Table 3).

We proceeded to test whether $^{m}\log D_{\mathrm{pr/pl}}$ might correlate more strongly with measured lipophilicity ($^{m}\log D$). For both monkey and human, strong and highly significant linear correlations were found between $^{m}\log D_{\mathrm{pr/pl}}$ and $^{m}\log D$ (Fig. 3; Table 2, entries 11 and 12). For human, the quantitative relationship was found to be

$$^{m}\log D_{\mathrm{pr/pl}} = 0.733\,^{m}\log D - 0.651 \quad (r^2 = 0.738; P < 0.0001) \qquad (1)$$

and for monkey,

$$^{m}\log D_{\mathrm{pr/pl}}=0.780\,^{m}\log D-1.15\,(r^{2}=0.832;P<0.0001) \quad (2)$$

Therefore, the use of $^{m}\log D$ in place of computed values resulted in much improved sensitivity (higher slope or correlation coefficient) and also in much stronger correlation (higher r^2). Equations 1 and 2 may be algebraically transformed to give the following relations between f_P and D for human and monkey, respectively.

$$f_P=1/(1+0.243D^{0.733}) \quad (3)$$

$$f_P=1/(1+0.0708D^{0.780}) \quad (4)$$

Species differences are important considerations in drug development and also in our research area of PET radiotracer development, where results in animals, usually rodents or monkeys, inform decisions on whether to advance radiotracer evaluations into humans. Only a few previous studies have compared f_P for drug-like compounds among species.[13,19,40,41] Comparison of the monkey and human f_P data for 14 of the 18 compounds in this study showed statistically significant species differences ($P < 0.05$) for five compounds (Table 1). In all five cases, f_P was lower in human than in monkey. The small set of other published studies also consistently reported lower f_P in human than in other species.[13,19,40,41] We found that the regression lines from the $^{m}\log D$ and $^{m}\log D_{\mathrm{pr/pl}}$ values for human and monkey were significantly different by covariance analysis ($P < 0.006$). The monkey data show the higher coefficients of regression and correlation and this may have a strong biological basis. Thus, the managed monkey population, from which the data in this study were obtained, is more homogeneous with regard to factors that include genetics, gender, diet, fasting state, absence of disease, and exposure to medications than the sampled humans. Such factors are well known to affect the binding of drugs to plasma proteins.[7,8] Moreover, there are documented intrinsic species differences in the nature of drug binding sites for serum albumin,[42–44] the most abundant drug-binding protein in blood,[7,8] and also for serum α_1-acid glycoprotein.45 Table 4 compares the linear relationships between $^{m}\log D_{\mathrm{pr/pl}}$ and $^{m}\log D$ established in this study for neutral and basic compounds in monkey and human (Eqs 1 and 2) with those established by Lázníček et al.[13] for low molecular weight carboxylic acids in several species (mouse, rat, rabbit, and human). The regression coefficients (slopes m) for the relationships established by Lázníček et al.[13] (Table 4, entries 1–4) are approximately 1 and significantly higher than for the relationships that we obtained for neutral and basic compounds in monkey and human (Table 4, entries 5 & 6). Acidic compounds are generally considered to bind preferentially to serum albumin whereas basic compounds are considered to bind preferentially to the much less abundant serum α_1-acid glycoprotein.[2,7,8] The differences in slopes between the equations obtained by Lázníček et al.[13] for acid compounds and those for the regression lines expressed in Eqs. 1 and 2 may reflect these general differences in acid/base binding preference as well as species differences in protein binding sites.

A high proportion of our set of neutral/basic compounds, eight from 18, contains one or more fluorine atoms. Fluorine atoms are known to confer unusual and even unexpected partition properties in small organic molecules.[46] Highly fluorinated molecules tend to be neither oil nor water soluble, and are often therefore described as fluorophilic. Because the presence of fluorine atoms in a molecule may cause lipophilicity and hydrophobicity to diverge, $\log P$ may not truly reflect lipophilicity.[47] Even incorporation of a low number of fluorine atoms into a drug-like molecule may have major consequences for disposition or protein binding. In view of these considerations, we examined the impact of removing the

eight fluorine-containing compounds from our datasets. For both human and monkey, this removal resulted in enhanced correlations of $^{m}\log D_{pr/pl}$ with $^{m}\log D$ (Fig. 4; Table 2, entries 11 & 12), with the monkey data again showing the stronger correlation. The correlations for the dataset of fluorine-containing compounds were much weaker (Fig. 4; Table 2, entries 13 & 14). The data for the fluorine compounds happen to appear mainly on the high side of the range of $^{m}\log D_{pr/pl}$ and $^{m}\log D$ values and show more dispersion about the regression line than for the nonfluorine-containing compounds. This may explain the observed differences in the strength of correlations of fluorine-containing and nonfluorine-containing compounds. Covariance analysis showed no statistical difference between the regression lines for fluorine-containing and non-fluorine-containing compound datasets ($P = 0.563$ for monkey and $P = 0.482$ for human).

The correlation coefficient for the relationship between monkey $^{m}\log D_{pr/pl}$ and $^{m}\log D$ for the structurally noncongeneric dataset of nonfluorinated compounds is remarkably high ($r^2 = 0.906$; $n = 10$) (Table 2). This implies that the two-phase *n*-octanol-pH 7.4 buffer system is an exceptionally robust model for the single-phase partition of compounds between plasma proteins and the remainder of plasma, and accounts for about 90% of this partition. It is useful to reflect on the meaning of the parameter $\log D_{pr/pl}$. In the hypothetical case of a compound binding to a single binding site in only one protein in plasma, $D_{pr/pl}$ would relate by the law of mass action to the equilibrium binding constant K_A, according to the expression:

$$K_A = D_{pr/pl}/[\text{protein}] \quad (5)$$

where [protein] is the protein concentration and therefore with f_P by:

$$K_A = ((1-f_P)/f_P)/[\text{protein}] \quad (6)$$

In pharmacology, ligand affinity to a protein is usually expressed as the equilibrium dissociation constant K_D, the reciprocal of K_A, with a low value representing high affinity binding. From Eqs. 5 and 6, it follows that K_D relates to $D_{pr/pl}$ by the expression:

$$K_D = [\text{protein}]/D_{pr/pl} \quad (7)$$

and therefore with f_P by:

$$K_D = [\text{protein}]/((1-f_P)/f_P) \quad (8)$$

For a low f_P value of 0.01 for a compound binding to a protein present at 0.6 mM, such as albumin in blood,[7,8] the K_D would be 6 μM[16] and for binding to the much less prevalent serum α_1-acid glycoprotein, with a typical blood concentration of ~20 μM,[8] the K_D would be 0.2 μM. These equilibrium dissociation constants are consistent with being due to relatively weak nonspecific interactions compared with the strong specific interactions of ligands that are needed for binding to proteins with K_D values in the nanomolar or even subnanomolar range. For example, in an extreme case, SP203 (**4**) binds specifically to metabotropic glutamate subtype five receptors with 37 pM affinity.[23] Of the ligands listed in Table 1, all f_P values exceed 0.0037, and they therefore bind to blood proteins with relatively low affinity.

As mentioned in the Introduction, different studies have reported different mathematical relationships between lipophilicity and f_p. Some are linear[4,15] and some are sigmoidal,[14] plus some are of the logarithmic type reported here (Eqs. 1 and 2).[13] The sigmoidal

relationships between f_P (or $1-f_P$) and log$D$ are in fact congruent with the logarithmic relationships because a plot of $\log_{10}[(1-f_p)/f_p]$ versus f_p is sigmoidal.[10] The linear relationship reported by Laruelle et al.[4] is for only four structurally congeneric and similarly basic compounds ([^{11}C]DASB (**5**) and congeners) covering a narrow log$D$ range of 2.44–3.31. Re-expression of the data as $^m\log D_{pr/pl}$ versus log$D$ actually improves the correlation coefficient (from $r^2 = 0.93$ to 0.98) and the statistical significance of the correlation from $P = 0.035$ to 0.011. In fact, there is no physical basis for expecting a linear relationship between f_P and lipophilicity (log$D$ or log$P$). Therefore, the poor linear relationship reported by Saiakhov et al.[15] ($r^2 = 0.29$, $n = 154$) is, in fact, as would be expected.

Do the quantitative relationships between compound log$D$ and f_P, derived from our model, have practical value? The relationships have some practical limitations. First, at least 10% of the variance in f_p is not accounted for by lipophilicity (log$D$). Second, small errors in the estimation or measurement of log$D$ can lead to sizable errors in the estimation of f_p. Because of the sigmoidal relationship between f_P and log$D$, the relative magnitude of the error in f_p depends on the true value of log$D$. Our set of PET brain-imaging radiotracers has f_p values in human that range widely from 0.44 for radiotracer **1** to 0.0037 for radiotracer **18** (Table 1). By Eq. 3, a compound with a log$D$ value of 0.816 would be expected to give an f_p value in human of 0.5. A +0.1 $\log_{10}$ unit error in the log$D$ value would predict an f_p value of 0.4999, that is, a negligible error in f_p. However, for very low values of f_p, errors become much more appreciable for the same error in log$D$. Thus, a compound with a log$D$ value of 3.869 would be expected to give an f_p value of 0.005. A +0.1 $\log_{10}$ unit error in the log$D$ value would predict an f_p value of 0.0042, that is, a −16% error in f_p. In most cases, we measured log$D$ with errors of <0.1 log10 unit (Table 1). Hence, $^m\log D$ values might be used to estimate f_p with reasonable accuracy, especially for moderate values. Although, from a practical standpoint, it may be just as easy to measure f_p as to measure log$D$, even with a nonradioactive compound, measurement of log$D$ may be more convenient because f_P measurement requires regulatory approvals for animal or human blood sampling. As experienced here, present computational methods for estimating log$D$ give sizeable root mean squared errors (≈0.8 $\log_{10}$ units). Major advances are therefore still needed in the accuracy of computational estimations of log$D$ for f_p in any species of interest to be predictable with good reliability.

CONCLUSIONS

For the set of structurally diverse nonacidic drug-like compounds studied here, $^m\log D$ accounts for over 73% of $^m\log D_{pr/pl}$ in humans and over 83% in monkey, despite the great structural dissimilarity between *n*-octanol and plasma proteins. The derived linear relationships (Eqs. 1 and 2) are statistically different between species. With the exception of one value among 13, monkey f_P values were consistently higher than human values. The much weaker correlation of $^m\log D_{pr/pl}$ with $^c\log D$ reflects appreciable errors intrinsic to computation of $^c\log D$ and points to the present limited value of computed lipophilicity for the development of *in-silico* methods for the prediction of f_P.

Acknowledgments

This research was supported by the Intramural Research Program of the National Institutes of Health (NIMH). The authors are grateful to Mr. J. Hong, Ms. C.L. Morse, Dr. Y. Zhang, and Dr. E. Luong for radiotracer syntheses, and to the NIH Clinical PET Center (Chief Dr. P. Herscovitch) for radioisotope production.

References

1. Smith, DA.; van de Waterbeemd, H.; Walker, DK. Pharmacokinetics and metabolism in drug design. Weinheim, Germany: Wiley VCH; 2001.

2. Schmidt S, Gonzalez D, Derendof H. Significance of protein binding in pharmacokinetics and pharmacodynamics. J Pharm Sci. 2010; 99:1107–1122. [PubMed: 19852037]
3. Waterhouse RN. Determination of lipophilicity and its use as a predictor of blood-brain barrier penetration of molecular imaging agents. Mol Imaging Biol. 2003; 5:376–389. [PubMed: 14667492]
4. Laruelle M, Slifstein M, Huang Y. Relationships between radiotracer properties and image quality in molecular imaging of the brain with positron emission tomography. Mol Imaging Biol. 2003; 5:363–375. [PubMed: 14667491]
5. Pike VW. PET radiotracers: Crossing the blood-brain barrier and surviving metabolism. Trends Pharmacol Sci. 2009; 30:431–440. [PubMed: 19616318]
6. Innis RB, Cunningham VJ, Delforge J, Fujita M, Gjedde A, Gunn RN, Holden J, Houle S, Huang SC, Ichise M, Iida H, Ito H, Kimura Y, Koeppe RA, Knudsen GM, Knuuti J, Lammertsma AA, Laruelle M, Logan J, Maguire RP, Mintun MA, Morris ED, Parsey R, Price JC, Slifstein M, Sossi V, Suhara T, Votaw JR, Wong DF, Carson RE. Consensus nomenclature for in vivo imaging of reversibly binding radioligands. J Cereb Blood Flow Metab. 2007; 27:1533–1539. [PubMed: 17519979]
7. Wilkinson GR. Plasma and tissue binding considerations in drug disposition. Drug Metab Rev. 1983; 14:427–465. [PubMed: 6347593]
8. Israeli ZH, Dayton PG. Human alpha-1-glycoprotein and its interactions with drugs. Drug Metab Rev. 2001; 33:161–235. [PubMed: 11495502]
9. van de Waterbeeemd H, Gifford E. ADMET *in silico* modeling: Towards prediction paradise. Nat Rev Drug Discov. 2003; 2:192–204. [PubMed: 12612645]
10. Hall LM, Hall LH, Kier LB. Methods for predicting the affinity of drugs and drug-like compounds for human plasma proteins: A review. Curr Comput Aided Drug Des. 2009; 5:90–105.
11. Leo A, Hansch C, Elkins D. Partition coefficients and their uses. Chem Rev. 1971; 71:525–616.
12. Smith RN, Hansch C, Ames MM. Selection of a reference partitioning system for drug design work. J Pharm Sci. 1975; 64:599–606. [PubMed: 1142068]
13. Lázníček M, Květina J, Mazák J, Krch V. Plasma protein binding-lipophilicity relationships: Interspecies comparison of some organic acids. J Pharm Pharmacol. 1987; 3:79–83. [PubMed: 2882008]
14. van de Waterbeemd H, Smith DA, Jones BC. Lipophilicity in PK design: Methyl, ethyl, futile. J Comput Aided Mol Des. 2001; 15:273–286. [PubMed: 11289080]
15. Saiakhov RD, Stefan LR, Klopman G. Multiple computer-automated structure evaluation model of the plasma protein binding affinity of diverse drugs. Perspectives Drug Discovery Des. 2000; 19:133–155.
16. Yamazaki K, Kanaoka M. Computational prediction of the plasma protein-binding percent of diverse pharmaceutical compounds. J Pharm Pharmacol. 2004; 93:1480–1494.
17. Kratochwil NA, Huber W, Muller F, Kansy M, Gerber PR. Predicting plasma protein binding of drugs: A new approach. Biochem Pharmacol. 2002; 64:1355–1374. [PubMed: 12392818]
18. Lobell M, Sivarajah V. In silico prediction of aqueous solubility, human plasma protein binding and volume of distribution of compounds from calculated pKa and AlogP98 values. Mol Diversity. 2003; 7:69–87.
19. Gleeson MP. Plasma protein binding affinity and its relationship to molecular structure: An in-silico analysis. J Med Chem. 2007; 50:101–112. [PubMed: 17201414]
20. Kumar JS, Prabhakaran J, Majo VJ, Milak MS, Hsiung S-C, Tamir S, Simpson NR, Van Heertum RL, Mann JJ, Parsey RV. Synthesis and in vivo evaluation of a novel 5-HT_{1A} receptor agonist radioligand [*O-methyl*-^{11}C]2-(4-(4-(2-methoxyphenyl)piperazin-1-yl)butyl)-4-methyl-1,2,4-triazine-3,5(2*H*,4*H*)dione in nonhuman primates. Eur J Nucl Med Mol Imaging. 2007; 34:1050–1060. [PubMed: 17221184]
21. Xu R, Hong J, Morse CL, Pike VW. Synthesis, structure-affinity relationships, and radiolabeling of selective high-affinity 5-HT_4 receptor ligands as prospective imaging probes for positron emission tomography. J Med Chem. 2010; 53:7035–7047. [PubMed: 20812727]
22. Fujita M, Zoghbi SS, Crescenzo MS, Hong J, Musachio JL, Lu J-Q, Lio J-S, Seneca N, Tipre DN, Cropley VL, Imaizumo M, Gee AD, Seidel J, Green MV, Pike VW, Innis RB. Quantification of

brain phosphodiesterase 4 in rat with (*R*)[^{11}C]rolipram-PET. NeuroImage. 2005; 26:1201–1210. [PubMed: 15961054]

23. Siméon FG, Brown AK, Zoghbi SS, Patterson VM, Innis RB, Pike VW. Synthesis and simple^{18}F-labeling of 3-fluoro-5-(2-(2-(fluoromethyl)thiazol-4-yl)ethynyl)benzonitrile as a high affinity radioligand for imaging monkey brain metabotropic glutamate subtype-5 receptors with positron emission tomography. J Med Chem. 2007; 50:3256–3266. [PubMed: 17571866]
24. Ichise M, Vines DC, Gura T, Anderson GM, Suomi SJ, Higley JD, Innis RB. Effects of early life stress on [^{11}C]DASB positron emission tomography imaging of serotonin transporters in adolescent peer- and mother-reared rhesus monkeys. J Neurosci. 2006; 26:4638–4643. [PubMed: 16641244]
25. Lu S, Liow JS, Zoghbi SS, Gladding RL, Innis RB, Pike VW. Evaluation of [^{18}F]SL702 as a prospective agonist PET radioligand for brain 5-HT$_{1A}$receptors in mice and monkey. NeuroImage. 2008; 41:T157.
26. Lazarova N, Zoghbi SS, Hong J, Seneca N, Tuan E, Gladding RL, Liow J-S, Taku A, Innis RB, Pike VW. Synthesis and evaluation of [*N-methyl*-^{11}C]*N*-desmethyl-loperamide as a new and improved PET radiotracer for imaging P-gp function. J Med Chem. 2008; 51:6034–6043. [PubMed: 18783208]
27. Zoghbi SS, Shetty HU, Ichise M, Fujita M, Imaizumi M, Liow JS, Shah J, Musachio JL, Pike VW, Innis RB. PET imaging of the dopamine transporter with^{18}F-FECNT: A polar radiometabolite confounds brain radioligand measurements. J Nucl Med. 2006; 47:520–527. [PubMed: 16513622]
28. Bao X, Lu S, Liow J-S, Zoghbi SS, Jenko KJ, Clark DT, Morse CL, Gladding RL, Innis RB, Pike VW. Radiolabeling and evaluation of [^{18}F]XB-1 in monkey as a prospective histamine subtype 3 receptor PET radioligand. J Label Compd Radiopharm (in press). 2011; 54(Suppl 1):S83.
29. Briard E, Zoghbi SS, Imaizumi M, Gourley JP, Shetty HU, Lu S, Fujita M, Innis RB, Pike VW. Synthesis and evaluation in monkey of two sensitive^{11}C-labeled aryloxyanilide ligands for imaging brain peripheral benzodiazepine receptors in vivo. J Med Chem. 2008; 51:17–30. [PubMed: 18067245]
30. Zoghbi SS, Liow JS, Yasuno F, Hong J, Tuan E, Lazarova N, Gladding RL, Pike VW, Innis RB. ^{11}C-Loperamide and its *N*-desmethyl radiometabolite are avid substrates for brain permeability-glycoprotein efflux. J Nucl Med. 2008; 49:649–656. [PubMed: 18344435]
31. McCarron JA, Zoghbi SS, Shetty HU, Vermeulen ES, Wikström HV, Ichise M, Yasuno F, Halldin C, Innis RB, Pike VW. Synthesis and initial evaluation of [^{11}C](*R*)-RWAY in monkey - a new, simply labeled antagonist radioligand for imaging brain 5-HT$_{1A}$receptors with PET. Eur J Nucl Med Mol Imaging. 2007; 34:1670–1682. [PubMed: 17579853]
32. Pike VW, Rash KS, Chen Z, Pedregal C, Statnick MA, Kimura Y, Hong J, Zoghbi SS, Fujita M, Toledo MA, Diaz N, Gackenheimer SL, Tauscher JT, Barth VN, Innis RB. Synthesis and evaluation of radioligands for imaging brain nociceptin/orphanin FQ peptide (NOP) receptors with positron emission tomography. J Med Chem. 2011; 54:2687–2700. [PubMed: 21438532]
33. Kreisl WC, Fujita M, Fujimura Y, Kimura N, Jenko KJ, Kannan P, Hong J, Morse CL, Zoghbi SS, Gladding RL, Jacobson S, Oh U, Pike VW, Innis RB. Comparison of [^{11}C]-(*R*)-PK 11195 and [^{11}C]PBR28, two radioligands for translocator protein (18 kDa) in human and monkey: Implications for positron emission tomographic imaging of this inflammation biomarker. NeuroImage. 2010; 49:2924–2932. [PubMed: 19948230]
34. Briard E, Zoghbi SS, Siméon FG, Imaizumi M, Gourley JP, Shetty HU, Lu S, Fujita M, Innis RB, Pike VW. Single-step high-yield radiosynthesis and evaluation of a sensitive^{18}F-labeled ligand for imaging brain peripheral benzodiazepine receptors with PET. J Med Chem. 2009; 52:688–699. [PubMed: 19119848]
35. Lu S, Liow JS, Zoghbi SS, Hong J, Innis RB, Pike VW. Evaluation of [^{11}C]S14506 and [^{18}F]S14506 in rat and monkey as agonist PET radioligands for brain 5-HT$_{1A}$receptors. Curr Radiopharm. 2010; 3:9–18. [PubMed: 20657759]
36. Donohue SR, Krushinski JH, Pike VW, Chernet E, Phebus L, Chesterfield AK, Felder CC, Halldin C, Schaus JM. Synthesis, ex vivo evaluation, and radiolabeling of potent 1,5-diphenylpyrrolidin-2-one cannabinoid subtype-1 receptor ligands as candidates for in vivo imaging. J Med Chem. 2009; 51:5833–5842. [PubMed: 18800770]

37. Clark, J.; Baldwin, R.; Bayne, K.; Brown, MJ.; Gebhart, GF.; Gonder, JC.; Gwathmey, JK.; Keeling, ME.; Kohn, DF.; Bobb, JW.; Smith, OA.; Steggerda, JA-D.; Van de Ber, JL. Guide for the Care and Use of Laboratory Animals, Institute of Laboratory Animal Resources. Washington, DC: National Research Council; 1996.
38. Gandelman MS, Baldwin RM, Zoghbi SS, Zea-Ponce Y, Innis RB. Evaluation of ultrafiltration for the free-fraction determination of single photon emission computed tomography (SPECT) radiotracers: β-CIT, IBF, and iomazenil. J Pharm Sci. 1994; 83:1014–1019. [PubMed: 7965658]
39. Tetko IV, Poda GI. Application of ALOGPS 2.1 to predict log*D* distribution coefficient for Pfizer proprietary compounds. J Med Chem. 2004; 47:5601–5604. [PubMed: 15509156]
40. Acharya MR, Sparreboom A, Sausville EA, Conley BA, Doroshow JH, Venitz J, Figg WD. Interspecies differences in plasma protein binding of MS-275, a novel histone deacetylase inhibitor. Cancer Chemother Pharmacol. 2006; 57:275–281. [PubMed: 16028097]
41. Kratochwil NA, Huber W, Muller F, Kansy M, Gerber PR. Predicting plasma protein binding of drugs–revisited. Curr Opin Drug Discov Devel. 2004; 7:507–511.
42. Kosa T, Maruyama T, Otagiri M. Species differences of serum albumins: I. Drug binding sites. Pharm Res. 1997; 14:1607–1612. [PubMed: 9434282]
43. Kosa T, Maruyama T, Otagiri M. Species differences of serum albumins: II. Chemical and thermal stability. Pharm Res. 1998; 15:449–454. [PubMed: 9563076]
44. Kosa T, Maruyama T, Sakai N, Yonemura N, Yahara S, Otagiri M. Species differences of serum albumins: III. Analysis of structural characteristics and ligand binding properties during N-B transitions. Pharm Res. 1998; 15:592–598. [PubMed: 9587956]
45. Matsumoto K, Sukimoto K, Nishi K, Maruyama T, Suenaga A, Otagiri M. Characterization of ligand binding sites on the α_1-acid glycoprotein in human, bovines and dogs. Drug Metab Pharmacokinet. 2002; 17:300–306. [PubMed: 15618681]
46. Goss KU, Bronner G. What is so special about the sorption behavior of highly fluorinated compounds? J Phys Chem A. 2006; 110:9518–9522. [PubMed: 16869704]
47. Bégué, J-P.; Bonnet-Delpon, D. Bioorganic and medicinal chemistry of fluorine. New Jersey: John Wiley & Sons, Inc; 2008.

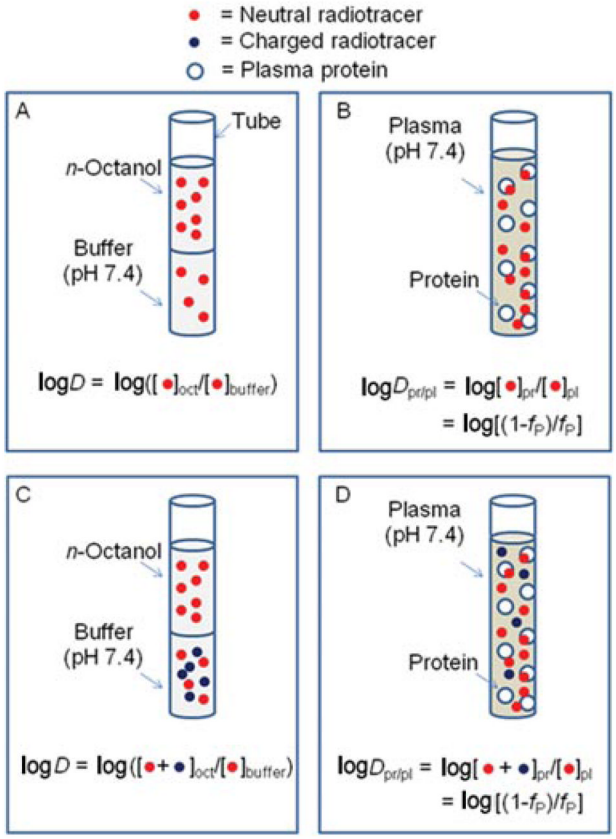

Figure 1.

Diagram illustrating the analogy between log*D* (partition of radiotracer between *n*-octanol and pH 7.4 buffer) and $\log D_{pr/pl}$ (partition of radiotracer between dissolved plasma proteins and remaining plasma) for neutral radiotracer (panels A and B) and for a basic radiotracer having protonated species at pH 7.4 (panels C and D). The models assume that charged species are excluded from *n*-octanol and from binding to plasma proteins.

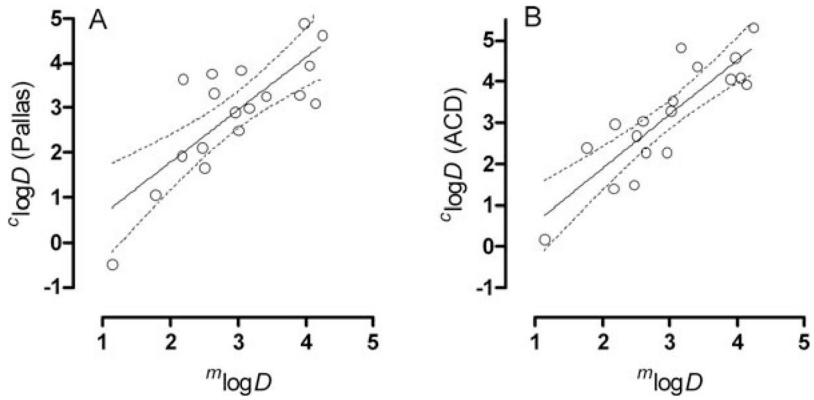

Figure 2.

Plots of $^{c}\log D$ from Pallas software (panel A) and ACD software (panel B) versus $^{m}\log D$ for the radiotracers **1** – **18** showing the regression lines and bounds of 95% confidence. The regression lines are defined in Table 2.

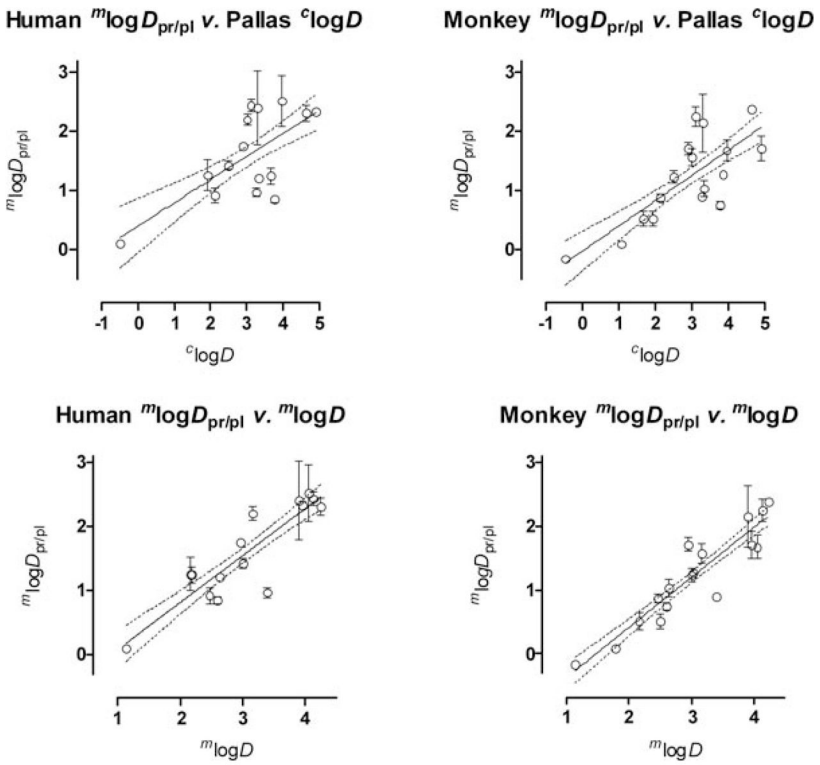

Figure 3.

$^{m}\log D_{pr/pl}$ versus $^{c}\log D$ and $^{m}\log D$ showing regression lines along with the 95% confidence intervals for human and monkey plasma samples. Where error bars are not visible they are within the symbol size. The regression lines are defined in Table 2.

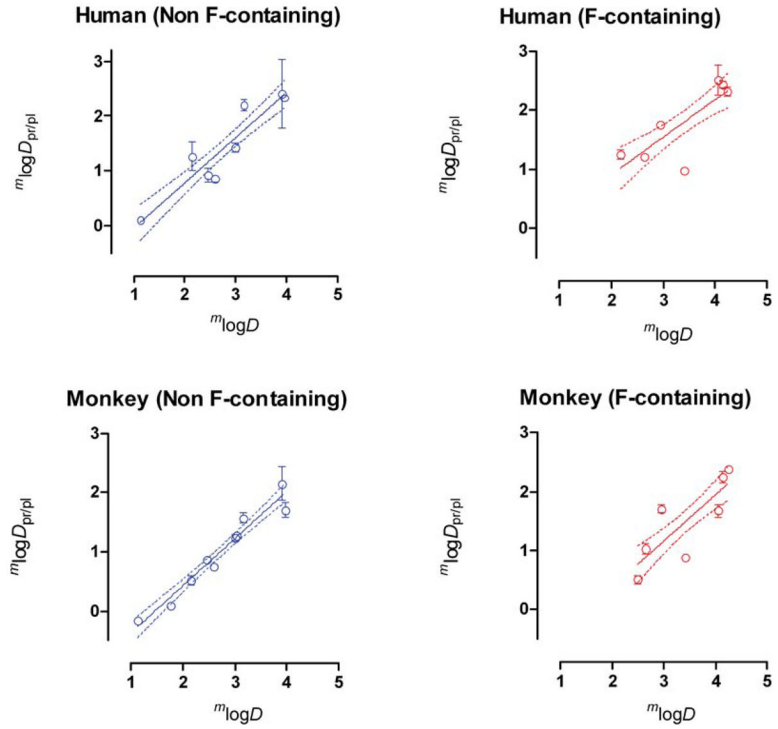

Figure 4.

Regression lines for human and monkey $^{m}\log D_{pr/pl}$ versus $^{m}\log D$ for fluorine-containing radiotracers and nonfluorine-containing radiotracers. Where error bars are not visible they are within the symbol size. The regression lines are defined in Table 2.

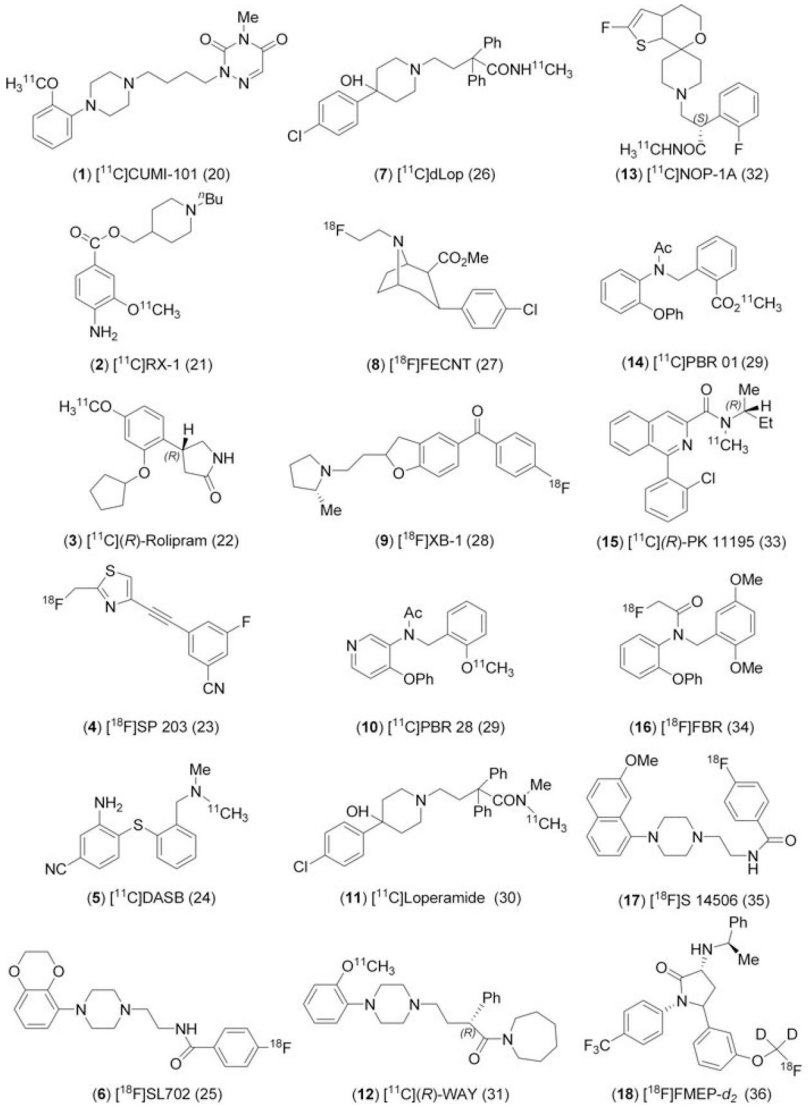

Chart 1.

Structures of radiotracers (**1** – **18**) used in this study. References to the radiotracers are given in parentheses.

Table 1

Measured and Computed Properties of Radiotracers **1 – 18**, Listed in Ascending Order of $^{m}\log D$

					$^{c}\log P$		$^{c}\log D$			f_P		$^{m}\log D_{pr/pl}$	
Entry	**Radiotracer**	**M. wt.**[a]	**tPSA**[b] **(Å)**	**pK_a**[c]	**Pallas**	**ACD**	**Pallas**	**ACD**	**$^{m}\log D$**[d]	**Monkey**[e]	**Human**[e]	**Monkey**[e]	**Human**[e]
1	[^{11}C]CUMI-101	372.5	56	9.25 9.13	1.49	0.00	−0.47	−0.19	1.13 ± 0.02	0.594 ± 0.016	0.442 ± 0.003*	−0.165 ± 0.029	0.101 ± 0.006*
2	[^{11}C]RX-1	320.5	65	8.47	2.16	2.62	1.06	2.39	1.77 ± 0.01	0.450 ± 0.0289	ND	0.087 ± 0.051	ND
3	[^{11}C](*R*)-Rolipram	275.3	48	7.61	2.35	1.41	1.93	1.41	2.16 ± 0.01	0.238 ± 0.0545	0.0580 ± 0.0327*	0.512 ± 0.132	1.26 ± 0.26*
4	[^{18}F]SP203	260.2	36	0.39	3.66	2.97	3.66	2.97	2.18 ± 0.22	ND	0.0550 ± 0.0165	ND	1.25 ± 0.13
5	[^{11}C]DASB	283.4	34	7.28	2.37	2.87	2.12	1.49	2.47 ± 0.02	0.120 ± 0.015	0.109 ± 0.029	0.868 ± 0.063	0.921 ± 0.124
6	[^{18}F]SL702	385.4	54	8.39	2.70	2.69	1.67	2.68	2.50 ± 0.01	0.238 ± 0.052	ND	0.511 ± 0.122	N.D.
7	[^{11}C]dLop	463.0	53	8.05	4.51	3.71	3.77	3.04	2.60 ± 0.04	0.154 ± 0.018	0.123 ± 0.015	0.742 ± 0.063	0.853 ± 0.060
8	[^{18}F]FECNT	325.8	30	6.99	3.47	3.31	3.33	2.28	2.64 ± 0.02	0.0873 ± 0.0255	0.0577 ± 0.0045	1.03 ± 0.14	1.21 ± 0.04
9	[^{18}F]XB-1	351.4	30	9.29	4.79	4.84	2.90	2.28	2.95 ± 0.01	0.0193 ± 0.0044	0.0175 ± 0.0014[f]	1.71 ± 0.11	1.75 ± 0.03[f]
10	[^{11}C]PBR28	348.4	51	6.58	2.56	3.30	2.50	3.29	3.01 ± 0.00	0.0560 ± 0.0125	0.0367 ± 0.0060	1.24 ± 0.11	1.42 ± 0.07
11	[^{11}C]Loperamide	477.0	44	8.01	4.55	4.26	3.85	3.53	3.04 ± 0.00	0.0512 ± 0.0036	ND	1.27 ± 0.11	ND
12	[^{11}C](*R*)-WAY	435.6	36	8.66	4.29	5.00	3.01	4.83	3.16 ± 0.35	0.0273 ± 0.0097	0.0063 ± 0.0015*	1.57 ± 0.15	2.20 ± 0.10*
13	[^{11}C]NOP-1A	420.5	42	7.47	3.61	5.21	3.27	4.36	3.41 ± 0.07	0.114 ± 0.005	0.0977 ± 0.0152	0.892 ± 0.02	0.969 ± 0.074
14	[^{11}C]PBR01	375.4	56	4.40	3.29	4.06	3.29	4.06	3.90 ± 0.02	0.0098 ± 0.0075	0.0072 ± 0.0086	2.15 ± 0.49	2.41 ± 0.620
15	[^{11}C](*R*)-PK11195	352.9	33	3.53	4.89	4.58	4.89	4.58	3.97 ± 0.18	0.0207 ± 0.0085	0.0047 ± 0.0006*	1.71 ± 0.21	2.33 ± 0.06*
16	[^{18}F]FBR	395.4	48	4.99	3.96	4.09	3.95	4.09	4.05 ± 0.02	0.0217 ± 0.0078	0.0040 ± 0.0030*	1.68 ± 0.18	2.52 ± 0.44*
17	[^{18}F]S14506	392.5	33	8.39	4.14	4.08	3.11	3.93	4.14 ± 0.06	0.0059 ± 0.0023	0.0037 ± 0.0009[f]	2.25 ± 0.17	2.44 ± 0.11[f]
18	[^{18}F]FMPEP- d_2	474.5	42	6.86	4.74	5.36	4.63	5.32	4.24 ± 0.08	0.0041 ± 0.0001	0.0050 ± 0.0017	2.39 ± 0.01	2.31 ± 0.14

*Significantly lower than monkey value ($P < 0.05$).

ND, not determined.

[a]For nonradioactive compound.

[b]Total polar surface area from Chem-Draw Ultra 11.0.

[c]Computed with Pallas 3.70; compound **1** has 2 values.

[d] Mean ± SD for $n = 6$.

[e] Mean ± SD for $n = 3$.

[f] Measured on pooled human plasma that had been stored at −70°C.

Table 2

Data from Regression Analyses of Dependent Variables Y and Independent Variables X, Where the Line is Defined as $Y = mX + c$, with m Representing Slope and c the Value of Y at $X = 0$

Entry	X	Y	n^a	m^b	c^b	$r^{2\,b}$	P^b
1	$^{m}\log D$	$^{c}\log D$ (Pallas)	18	1.17 ± 0.23	−0.544 ± 0.706	0.619	0.0001
2	$^{m}\log D$	$^{c}\log D$ (ACD)	18	1.31 ± 0.19	−0.736 ± 0.600	0.740	<0.0001
3	$^{c}\log D$ (ACD)	$^{m}\log D_{pr/pl}$ (human)	15	0.384 ± 0.053	0.352 ± 0.184	0.553	<0.0001
4	$^{c}\log D$ (ACD)	$^{m}\log D_{pr/pl}$ (monkey)	17	0.394 ± 0.045	−0.0365 ± 0.0498	0.561	<0.0001
5	$^{c}\log D$ (Pallas)	$^{m}\log D_{pr/pl}$ (human)	15	0.393 ± 0.070	0.394 ± 0.229	0.426	<0.0001
6	$^{c}\log D$ (Pallas)	$^{m}\log D_{pr/pl}$ (monkey)	17	0.428 ± 0.053	−0.0283 ± 0.168	0.569	<0.0001
7	$^{c}\log P$ (ACD)	$^{m}\log D_{pr/pl}$ (human)	15	0.351 ± 0.062	−0.292 ± 0.241	0.430	<0.0001
8	$^{c}\log P$ (ACD)	$^{m}\log D_{pr/pl}$ (monkey)	17	0.407 ± 0.050	−0.268 ± 0.193	0.574	<0.0001
9	$^{c}\log P$ (Pallas)	$^{m}\log D_{pr/pl}$ (human)	15	0.461 ± 0.089	−0.0674 ± 0.333	0.385	<0.0001
10	$^{c}\log P$ (Pallas)	$^{m}\log D_{pr/pl}$ (monkey)	17	0.504 ± 0.070	−0.571 ± 0.256	0.519	<0.0001
11	$^{m}\log D$	$^{m}\log D_{pr/pl}$ (human)	15	0.733 ± 0.067	−0.651 ± 0.212	0.738	<0.0001
12	$^{m}\log D$	$^{m}\log D_{pr/pl}$ (monkey)	17	0.780 ± 0.050	−1.15 ± 0.16	0.832	<0.0001
13	$^{m}\log D$	$^{m}\log D_{pr/pl}$ (human; fluoro)	7	0.635 ± 0.120	−0.364 ± 0.416	0.595	<0.0001
14	$^{m}\log D$	$^{m}\log D_{pr/pl}$ (monkey; fluoro)	7	0.784 ± 0.130	−1.19 ± 0.45	0.659	<0.0001
15	$^{m}\log D$	$^{m}\log D_{pr/pl}$ (human; nonfluoro)	8	0.824 ± 0.084	−0.870 ± 0.246	0.814	<0.0001
16	$^{m}\log D$	$^{m}\log D_{pr/pl}$ (monkey; nonfluoro)	10	0.798 ± 0.049	−1.17 ± 0.14	0.906	<0.0001

[a] n = number of data points used in regression analysis, with one data point per compound; means were used for measured values.

[b] Values computed with GraphPad Prism for Windows software.

Table 3

Comparison of m and c Values for Relationships $^{m}\log D_{pr/pl} = m\,^{c}\log P + c$ in Human and Monkey for Different Sources of $^{c}\log P$ and Organic Compound Classes

Entry	Species	Source of $^{c}\log P$	Compound class	n	r^2	m	c
1[a]	Human	Cerius2 (version 4.6)	Uncharged	78	0.63	0.449	−0.416
2[a]	Human	Cerius2 (version 4.6)	Positively charged	63	0.67	0.463	−1.097
3[b]	Human	ACD	Neutral/basic	15	0.430	0.351	−0.834
4[b]	Monkey	ACD	Neutral/basic	17	0.574	0.407	−0.268
5[b]	Human	Pallas 3.0	Neutral/basic	15	0.385	0.461	−0.067
6[b]	Monkey	Pallas 3.0	Neutral/basic	17	0.519	0.504	−0.571

[a] From Ref. 18.

[b] From this study.

Table 4

Comparison of m and c Values for Relationships $^{m}\log D_{pr/pl} = m^{m}\log D + c$ in Various Species and for Different Organic Compound Classes

Entry	Species	Compound class	*n*	r^2	*m*	*c*
1[a]	Mouse	Acidic	11	0.884	1.04	−2.15
2[a]	Rat	Acidic	11	0.931	1.01	−1.75
3[a]	Rabbit	Acidic	11	0.945	1.02	−1.28
4[a]	Human	Acidic	11	0.970	0.994	−1.10
5[b]	Monkey	Neutral/basic[c]	17	0.832	0.780	−1.15
6[b]	Human	Neutral/basic[c]	15	0.738	0.733	−0.651
7[b]	Monkey	F-noncontaining neutral/basic	10	0.906	0.798	−1.17
8[b]	Monkey	F-containing neutral/basic	7	0.659	0.784	−1.10
9[b]	Human	F-noncontaining neutral/basic	8	0.814	0.824	−0.870
10[b]	Human	F-containing neutral/basic	7	0.595	0.635	−0.364

[a] From Ref. 13.

[b] From this study.

[c] Includes fluorine-containing and nonfluorine-containing compounds.